TRANSACTIONS ON EMERGING TELECOMMUNICATIONS TECHNOLOGIES
Trans. Emerging Tel. Tech. 2015; **26**:670–685
Published online 25 August 2013 in Wiley Online Library (wileyonlinelibrary.com). DOI: 10.1002/ett.2698

RESEARCH ARTICLE

Energy and spectral efficiencies trade-off with filter optimisation in multiple access interference-aware networks

Álvaro R. C. Souza[1], Taufik Abrão[1]*, Lucas H. Sampaio[2], Paul Jean E. Jeszensky[2], Jordi Pérez-Romero[3] and Ferran Casadevall[3]

[1] Department of Electrical Engineering, State University of Londrina (UEL), Londrina, Parana 86051-970, PO Box 6001, Brazil
[2] Department of Telecommunication and Control Engineering, Escola Politécnica of the University of São Paulo (EPUSP), São Paulo, Brazil
[3] Department of Signal Theory and Communications, Universitat Politècnica de Catalunya (UPC), Barcelona, Spain

ABSTRACT

In this contribution, the optimised deployment of both spectrum and energy resources scarcely available in the mobile multiple access systems has been analysed, with special attention to the impact of the filter design on the energy efficiency (EE) of code division multiple access networks. Putting into perspective two conflicting metrics, namely throughput maximisation and power consumption minimisation, the distributed EE utility function is formulated. We also show that the best EE versus spectral efficiency trade-off is achievable when each node allocates exactly the power necessary to attain the maximum EE. In order to demonstrate the validity of our analysis, a low-complexity energy-spectral-efficient algorithm based on distributed instantaneous signal-to-interference-plus-noise ratio level is developed, and the impact of single and multi-user detection filters on the EE–spectral efficiency trade-off is extensively analysed by numerical simulation.

***Correspondence**
T. Abrão, Department of Electrical Engineering, State University of Londrina, Londrina, Parana 86051-970, PO Box 6001, Brazil.
E-mail: abrao@ieee.org; taufik@uel.br

Received 20 February 2013; Revised 5 June 2013; Accepted 6 June 2013

1. INTRODUCTION

Resource allocation techniques, mainly power optimisation, are becoming increasingly important in wireless system design, because battery technology evolution has not followed the explosive demand of mobile devices and environmental issues. Resource allocation problems in wireless networks are systematically treated in [1, Ch.4-6], aiming to maximise the sum of utilities of link rates for best-effort traffic. The methodology in [1, Ch.4-6] consists in identifying a class of utility functions for which the power control problem can be converted into an equivalent convex optimisation problem. The convexity property is a key ingredient in the development of powerful and efficient power control algorithms (PCAs).

One of the most interesting ways of dealing with the power allocation problem is the energy-efficiency (EE) approach [2–4], which aims to maximise the transmitted data per energy unit (measured in bits per Joule) and is closely related to green communication techniques [5]. Recent works in the field include the EE problem formulation in the context of multiple access networks, such as orthogonal frequency division multiple access (OFDMA) [4, 6] and code division multiple access (DMA) (CDMA) [3, 7], with particular interest in multi-carrier CDMA systems. The energy-efficient approach to CDMA system scenarios can include the jointly spreading-code and receiver optimisation [8]. On the receiver side, multi-user detection techniques could be included in order to reduce the multiple access interference (MAI) effects [7, 9]. As pointed out by Chen *et al*. [10], one of the most important trade-offs in green wireless communications is EE versus spectral efficiency (EE–SE) trade-off; the goal consists in balancing these two important metrics. In this context, one of the most important issues is the characterisation of the EE–SE trade-off in multi-user environments, such as OFDMA, CDMA and multi-carrier CDMA. In [11], the authors demonstrate that the EE–SE trade-off gap in OFDMA systems is reduced when interference increases, assuming some restrictions in users power and position.

The EE–SE trade-off through the use of designed utility functions and distributed mechanisms have been studied in [12]. In this context, the user's utility is a function of throughput and average transmission power, where throughput is assumed to be a sigmoidal function of signal-to-interference-plus-noise ratio (SINR), while power consumption function is admitted affine. The EE–SE optimisation problem has been formulated as a game, where each user, being selfish and rational, acts to maximise its utility in response to the SINR by adjusting its transmission power. The resulting mechanism is a distributed power control scheme that can incline towards energy-efficient or spectrally efficient operating points depending on the choice of utility function.

The relationship between EE and quality of service (QoS) in wireless networks has been investigated recently in various works. In [13], the authors show that there exist fundamental trade-offs between EE and quality of experience (QoE) for users with different traffics when transmission power and circuit power consumptions, interference and network bandwidth have been considered.

Because SE is a monotonic increasing function of the transmitting power level, in multiple access CDMA systems, which are limited by interference level, the SE is also constrained by the maximum transmitted power available at each network node. As a consequence, although the sum rate capacity (proportional to SE) increases with the number of active users, the level of interference generated, induced by new users sharing the same bandwidth, increases. Hence, on the one hand, the total network power consumption grows in order to achieve the optimum SINR, while, on the other hand, the EE is reduced in terms of transmitted bits per Joule units. One way to reduce the generated interference by the non-cooperative game approach is the use of pricing techniques [14]. Hence, users are stimulated to allocate less power, which implies lower interference.

This work proposes a power control procedure based on the optimised deployment of two main resources scarcely available in multiple access mobile terminals (MTs), that is, spectrum and energy, considering direct sequence CDMA (DS/CDMA) systems. Besides, the EE–SE trade-off behaviour is extensively characterised under different interference level scenarios. From the analysis of two conflicting metrics, namely throughput maximisation and power consumption minimisation, the distributed EE cost function is formulated as a non-cooperative game. Indeed, the overall EE of the network depends on the behaviour of each single user; thus, power control can be properly modelled as a non-cooperative game [15][8] [16] [11]. In this work, a non-cooperative game is applied to describe and to solve the EE–SE trade-off in wireless communication scenarios.

We also investigate the impact of multi-user detection schemes, motivated by the fact that the gap between the optimal EE and the maximal SE is reduced when the MAI increases. Because those detectors can mitigate the MAI from other users, their deployment could result in more energy-efficient systems. Furthermore, the paper shows that the best EE–SE trade-off is achievable when each node allocates exactly the power necessary to attain the maximum EE, while SE is determined by the attainable rate in each node. In order to demonstrate the validity of the proposal, a low-complexity energy-spectral-efficient algorithm based on distributed instantaneous SINR level is developed.

The main contributions of this work are threefold: (i) analysing the energy and spectral efficiencies in CDMA systems from the perspective of the two conflicting metrics, throughput maximisation and power level consumption minimisation; (b) evaluating the impact of the filter receiver choice over EE–SE trade-off; (c) discussing the peak power constraint on the performance and EE-SE trade-off as well. This paper is organised as follows. In Section 2, we define the system model. The EE–SE optimisation problem formulation is given in Section 3, and in Section 4, we discuss the effects of MAI on the EE–SE trade-off. In Section 5, we propose two algorithms to implement distinct metrics of the EE–SE trade-off optimisation; discussion on the numerical results is offered in Section 6. Finally, Section 7 brings the main conclusions.

2. NETWORK SYSTEM MODEL

For analysis simplicity, initially we assumed a single cell uplink DS/CDMA network with K MTs. However, the extension for multi-cell multi-carrier multiple access systems is straightforward [17,18]. The N-dimensional vector representing the equivalent baseband received signal in the base station (BS) can be described as follows:

$$\mathbf{y} = \sum_{k=1}^{K} \sqrt{p_k} h_k b_k \mathbf{s}_k + \boldsymbol{\eta} \tag{1}$$

where b_k is the modulated symbol; $h_k = |h_k| e^{\angle h_k}$ is the complex channel gain between the kth user and BS, assumed constant during the symbol period; $\mathbf{s}_k$ is the kth user spreading code vector with length $N = r_c/r$, representing the processing gain given by the ratio between chip rate (r_c) and symbol rate (r); and finally, $\boldsymbol{\eta}$ represents the thermal noise, assumed to be additive white Gaussian noise (AWGN), with zero-mean and covariance matrix given by $\sigma^2 \mathbf{I}_N$. We assume that fading is slow, flat and constant during optimisation window.

The SINR is defined by the ratio between the received signal power to the sum of interfering power plus background noise, measured after demodulation. In DS/CDMA, this ratio depends on the detection strategy. Considering the adoption of linear receivers, the SINR is given by [7]

$$\gamma_k = \frac{p_k \mathrm{h}_k \left(\mathbf{d}_k^T \mathbf{s}_k\right)^2}{\sum\limits_{j \neq k}^{K} p_j \mathrm{h}_j \left(\mathbf{d}_k^T \mathbf{s}_j\right)^2 + \sigma_k^2 \left(\mathbf{d}_k^T \mathbf{d}_k\right)} = \frac{p_k \mathrm{h}_k}{\mathcal{I}_k + \sigma_k^2 \left(\mathbf{d}_k^T \mathbf{d}_k\right)} \tag{2}$$

where $\mathrm{h}_k = |h_k|^2$ is the channel power gain, $\mathcal{I}_k = \sum_{j \neq k}^{K} p_j \mathrm{h}_j \left(\mathbf{d}_k^T \mathbf{s}_j\right)^2$ represents the MAI power level,

$\mathbf{s}_k = \frac{1}{\sqrt{N}}[c_1, c_2, \cdots, c_N]^T, c_i = \mathcal{U}\{-1, 1\}$ is the kth user pseudo-noise spreading code, with $(\mathbf{s}_k^T \mathbf{s}_k) = 1$, and $\mathbf{d}_k$ is the N-dimensional vector representing the receive filter for the kth user; $(\cdot)^T$ denotes the transpose operator.

To perform detection, we consider single-user and multi-user strategies. For the single-user detection (SuD), we deploy matched filter (MF). For this receiver, the filter vector $\mathbf{d}_k$ is defined as the kth user spreading code, and the interference power is regarded as background noise, which limits the system performance, because CDMA systems are limited by the interference level. Hence, the SINR expression for MF can be written as follows:

$$\gamma_k^{\mathrm{MF}} = \frac{p_k \mathrm{h}_k}{\sum\limits_{j \neq k}^{K} p_j \mathrm{h}_j \left(\mathbf{s}_k^T \mathbf{s}_j\right)^2 + \sigma_k^2} = \frac{p_k \mathrm{h}_k}{\mathcal{I}_k^{\mathrm{MF}}} \tag{3}$$

where $\mathcal{I}_k$ is the MAI plus background noise.

For the multi-user approach, we consider linear multi-user detectors [19], such as decorrelator (DEC), zero-forcing and the minimum mean square error (MMSE). Linear multi-user detectors are useful to power optimisation algorithms because the resulting SINR is deterministic, unlike heuristic-based methods, and that is important to find the minimum power to achieve the target SINR. Besides the better performance, the MMSE detector demands the amplitude matrix of all users, and we consider a distributed solution; thus, DEC detector has been deployed, which presents a slight inferior performance regarding the MMSE detector, but it depends only on the spreading codes ($\mathbf{s}_k$) and the correlation matrix $\mathbf{R}$ [7]. Both parameters are constant during the PCA execution, which requires just one transmission at the beginning of algorithm iterations. The DEC filter is given by

$$\mathbf{D}_{\mathrm{DEC}} = [\mathbf{d}_1\, \mathbf{d}_2\, \cdots\, \mathbf{d}_k\, \cdots\, \mathbf{d}_K] = \mathbf{S}\mathbf{R}^{-1} \tag{4}$$

Hence, the SINR achieved is

$$\gamma_k^{\mathrm{DEC}} = \frac{p_k \mathrm{h}_k}{\sigma^2 \mathbf{d}_k^T \mathbf{d}_k} = \frac{p_k \mathrm{h}_k}{\mathcal{I}_k^{\mathrm{DEC}}} \tag{5}$$

2.1. Quality of service requirements

In order to guarantee the QoS, a minimum data rate $R_{k,\min}$ must be provided for each user by system network service, being an important requirement to be guaranteed. The maximum achievable data rate can be obtained with Shannon capacity equation [20–22], given by

$$\mathcal{C}_k = \mathrm{w} \log_2(1 + \gamma_k) \qquad [\mathrm{bits}/s] \tag{6}$$

where w is the multiple access bandwidth.

Because the capacity in Equation (6) is a theoretical boundary, that is, the maximal achievable rate, it is relevant to include a gap factor capable to describe the limitations and imperfections in real communication systems, such as modulation effects. Hence, the Shannon capacity equation can be re-written as an approximation for the attainable data rate given a gap between the theoretical capacity curve and the real data rate [22]. Equivalently, this gap can be expressed through an effective SINR reduction:

$$\mathcal{C}_k^{\mathrm{gap}} = \mathrm{w} \log_2(1 + \theta_k \cdot \gamma_k), \qquad \forall k \qquad [\mathrm{bit}/s] \tag{7}$$

where $\theta_k = -\dfrac{1.5}{\ln(5\,\mathrm{BER}_k)}$, with $\theta_k \in [0; 1[$

BER_k is the maximum tolerable bit error rate by the kth user [23]. Thus, the SE is obtained from Equation (7):

$$\zeta_k = \log_2(1 + \theta_k \cdot \gamma_k), \qquad \forall k \qquad \left[\frac{\mathrm{bit}}{\mathrm{s} \cdot \mathrm{Hz}}\right] \tag{8}$$

Hence, the *attainable data rate* is readily obtained from the Shannon capacity, Equation (7), with appropriate detector filter:

$$R_k = \mathrm{w} \log_2\left(1 + \theta_k \cdot \gamma_k^{\mathrm{filter}}\right), \tag{9}$$

where $\gamma_k^{\mathrm{filter}}$ is given herein by Equation (3) or (5).

From Equation (9), the minimum data rate for the kth link, $R_{k,\min}$, which is able to guarantee the QoS, considering maximum tolerable BER for that service, can be easily mapped into the minimum SINR:

$$\gamma_{k,\min} = (2^{R_{k,\min}/\mathrm{w}} - 1)/\theta_k \qquad \forall k = 1, \ldots, K \tag{10}$$

In the next section, the EE–SE optimisation problem in multiple access networks is formulated taking into account many system parameters and functions, such as transmitted packets, circuit power consumption, SINR, error probability, energy and SE functions and efficiency function, as well as single and multi-user filter detection schemes.

3. PROBLEM FORMULATION

In an MAI limited communication system, the kth user selfishly (non-cooperative approach) allocates his own transmit power p_k and receive filter strategy (single-user or multi-user detection strategy) in order to maximise his own EE function, expressed by [24]:

$$\xi_k = r_k \frac{L}{M} \frac{f(\gamma_k)}{p_k + p_c} \qquad \left[\frac{\mathrm{bit}}{\mathrm{Joule}}\right], \qquad \forall k = 1, \ldots, K \tag{11}$$

where r_k in bits per second is the *transmission data rate*, which, in practice, is less than the attainable rate; M is the number of bits in each transmitted data packet; L is the number of information bits contained in each data packet; p_k is the transmission power; p_c is the circuit power consumption; and $f(\gamma_k)$ is the *efficiency function*, which approximates the probability of error-free packet reception, because the attainable data rate and the transmission data

Trans. Emerging Tel. Tech. **26**:670–685 (2015)
DOI: 10.1002/ett

rate are related by the probability of correct reception [24]. When no coding is used, the efficiency function can be approximated by [8]

$$f(\gamma_k) = (1 - \mathrm{BER}_k)^M \approx (1 - e^{-\gamma_k})^M \qquad (12)$$

Besides, the efficiency function approximation in Equation (12) was adopted in order to work with a well-behaved utility function; that is, this function has the desirable properties at the limiting points $\gamma_k = 0$ and $\gamma_k = \infty$ [7,25], while holding the same shape as the original utility function $f(\gamma_k) = (1 - \mathrm{BER}_k)^M$ [24].

It is worth noting that both transmission power and circuit power consumptions are very important factors for energy-efficient communications. While p_k is used for reliable data transmission, circuit power p_c represents the average energy consumption of electronics devices and circuitry [4]. Furthermore, the kth SINR admits different definitions depending on system type, detection strategy (SuD or LMuD), spreading sequence type and so forth. Note that ξ_k in Equation (11) is measured in bits per Joule, which represents the number of successful bit transmissions that can be made for each energy unit drained from the battery and effectively used for transmission.

In a more general context, we can define the concept of global EE function as the ratio of the total achievable capacity over the total power transmission consumption:

$$\bar{\xi} = \frac{\sum_{k=1}^{K} \ell_k r_k f(\gamma_k)}{P_{\mathrm{Tot}}} \qquad \left[\frac{\text{bit}}{\text{Joule}}\right] \qquad (13)$$

where $P_{\mathrm{Tot}} = p_c + \sum_{k=1}^{K} \varrho_k p_k$, and $\ell_k = \left(\frac{L}{M}\right)_k$, where $\varrho_k > 1$ is the power amplifier inefficiency associated to the kth transmitter.

3.1. Distributed non-cooperative energy efficiency power optimisation game

The network EE depends on the behaviour of all users; thus, the power control problem can be properly modelled as a non-cooperative game [15]. In the context of a non-cooperative power control game,

$$\mathcal{G} = [\mathcal{K}, \{\mathcal{A}_k\}, \{u_k\}] \qquad (14)$$

where $\mathcal{K} = \{1, 2, \ldots, K\}$ is the set of active users; $\{\mathcal{A}_k\} = [0, P_{\max}]$ is the strategy set for the kth user, with $P_{\max}$ being the maximum allowed power for transmission; and the utility functions $\{u_k\}$ are performed by the EE function ξ_k.

Considering the power allocation for the kth user, p_k, the power vector of other users (interfering users) can be denoted as [7]:

$$\mathbf{p}_{-k} = [p_1, p_2, \ldots, p_{k-1}, p_{k+1}, \ldots, p_K] \qquad (15)$$

Hence, given the power allocation of all interfering users, $\mathbf{p}_{-k}$, the best response of the power allocation for the kth user, p_k, can be expressed as follows:

$$p_k^{\mathrm{best}} = q_k(\mathbf{p}_{-k}) = \arg\max_{p_k} \; u_k(p_k, \mathbf{p}_{-k}) \qquad (16)$$

where u_k is given by Equation (11), and $q_k(\mathbf{p}_{-k})$ is called the kth best-response function.

Finally, the problem for distributed EE under non-cooperative game perspective can be posed as follows:

$$\begin{aligned} \arg\max_{p_k} \xi_k = \arg\max_{p_k} \quad & \ell_k r_k \frac{f(\gamma_k)}{p_k + p_c} \\ \text{s.t.} \quad & 0 \leqslant p_k \leqslant P_{\max} \end{aligned} \qquad (17)$$

whose solution consists in adopting the best-response strategy for the kth user. Indeed, the best-response strategy consists in obtaining the maximum EE individually for each user, as posed by Equation (16). Hence, we can find the optimum operation point by taking the first and second derivative tests, given the interfering power vector $\mathbf{p}_{-k}$.

3.2. Best signal-to-interference-plus-noise ratio response for single-user detection and linear multi-user detectors filters

The power allocation for kth user can be expressed as

$$p_k = \gamma_k \frac{\mathcal{I}_k^{\mathrm{filter}}}{\mathrm{h}_k} = \gamma_k \widetilde{I}_k^{\mathrm{filter}}, \qquad (18)$$

where $\widetilde{I}_k^{\mathrm{MF}} = \mathcal{I}_k^{\mathrm{MF}}/\mathrm{h}_k$ is the normalised interference plus noise at the MF output and $\widetilde{I}_k^{\mathrm{DEC}} = \mathcal{I}_k^{\mathrm{DEC}}/\mathrm{h}_k$ for DEC.

The first derivative of EE function ξ_k (17) regarding p_k is equivalent to taking the first derivative of ξ_k regarding γ_k [7], which results in

$$\frac{\partial \xi_k}{\partial \gamma_k} = \frac{\partial}{\partial \gamma_k} \left\{ \ell_k \frac{(1 - e^{-\gamma_k})^M \log(1 + \theta_k \gamma_k)}{\gamma_k \widetilde{\mathcal{I}}_k + p_c} \right\} \qquad (19)$$

with efficiency function given by Equation (12).

Hence, the optimal SINR for the kth user, γ_k^*, in terms of EE–SE trade-off is obtained by finding the solution of $\partial \xi_k / \partial \gamma_k = 0$ (maximisation point), admitting the normalised MAI $\widetilde{I}_k$ fixed. This condition is equivalent to solving function (20) regarding γ_k.

$$\begin{aligned} M e^{-\gamma_k} \log_2(1 + \theta_k \gamma_k) + \frac{\theta_k (1 - e^{-\gamma_k})}{(1 + \theta_k \gamma_k) \ln 2} = \\ \frac{\widetilde{\mathcal{I}}_k \log_2(1 + \theta_k \gamma_k)(1 - e^{-\gamma_k})}{(\gamma_k \widetilde{\mathcal{I}}_k + p_c)} \end{aligned} \qquad (20)$$

In order to guarantee that Equation (20) has only one maximiser, we introduce the concept of quasiconcavity, defined as follows[25]:

Definition 1 (Quasiconcavity). *A function z that maps a convex set of n-dimensional vectors $\mathcal{D}$ into a real number, i.e., $\mathbb{R}^n \mapsto \mathbb{R}$, is quasiconcave if for any $\mathbf{x}_1, \mathbf{x}_2 \in \mathcal{D}, \mathbf{x}_1 \neq \mathbf{x}_2$,*

$$z(\lambda \mathbf{x}_1 + (1-\lambda)\mathbf{x}_2) \geq \min\{z(\mathbf{x}_1), z(\mathbf{x}_2)\} \tag{21}$$

where $\lambda \in (0,1)$. The function z is said to be strictly quasiconcave if

$$z(\lambda \mathbf{x}_1 + (1-\lambda)\mathbf{x}_2) > \min\{z(\mathbf{x}_1), z(\mathbf{x}_2)\} \tag{22}$$

The proof of the strictly quasiconcavity of u_k is described in the Appendix, and the result is described by the next lemma:

Lemma 1 (Strictly quasiconcavity of u_k). *The utility function $u_k(p_k, \mathbf{p}_{-k})$ is strictly quasiconcave in p_k.*

This result is very important in the proof of existence and uniqueness of the system equilibrium, as discussed in the Appendix. With this lemma, we can guarantee that the utility function in Equation (17) has only one maximiser,* that is, the optimum SINR γ_k^* point where $\partial \xi_k / \partial \gamma_k = 0$; otherwise, if $\gamma_k^* > \gamma_k^{\max}$ for some k, where $\gamma_k^{\max}$ is the SINR associated to the maximum available power allocation, $P_{\max}$, then $P_{\max}$ will be deployed by the kth user, and the maximiser of the utility function could not be attained [25] [7] [8].

4. INTERFERENCE IMPACT ON THE ENERGY EFFICIENCY–SPECTRAL EFFICIENCY TRADE-OFF

In this section, we present a trade-off analysis between non-cooperative energy-efficient and spectral-efficient power control schemes.† This trade-off is determined by the MAI level, which accounts for *gap* Λ *among the maximal EE and the optimum SE* (only attainable with infinity power allocation). In realistic interference-aware systems, the increasing number of active users causes an increase of system capacity and simultaneously an increment in MAI. As a consequence, the SE of the system is able to increase accordingly. Defining this gap as the difference of the SE attainable at the maximal EE point (γ_k^{EE}) and that obtained deploying the maximal available power (i.e. the maximal achievable SE, γ_k^{SE}), we have

$$\Lambda = \zeta(\gamma_k^{\mathrm{SE}}) - \zeta(\gamma_k^{\mathrm{EE}}) \qquad \left[\frac{\text{bit}}{\text{s} \cdot \text{Hertz}}\right] \tag{23}$$

*$\gamma_k = 0$ also is a solution for Equation (20), but because $\forall p_k \in (0, P_{\max}], \xi_k > 0$, we can see that $\gamma_k = 0$ is a global minimum.

†Besides the fact that in low power regime the EE and SE are not conflicting metrics, our interest is in medium and high power regime, and in this operation condition, these two metrics are, in general, conflicting.

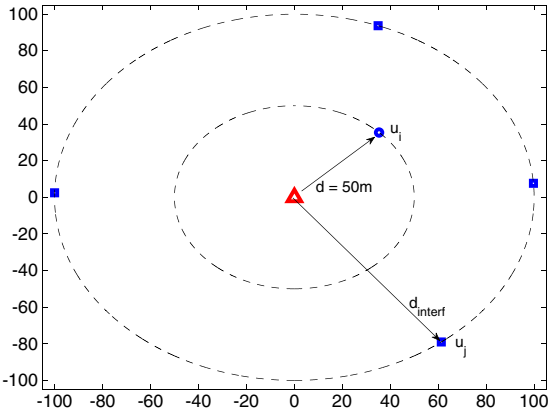

Figure 1. Cell geometry with increasing interference level, $I \propto d_{\mathrm{interf}}^{-\iota}$, $\iota \geq 2$.

On the other hand, it will be shown that gap Λ could be reduced when the interference level increases. Thus, in order to quantify this effect, we define the network topology as described in Figure 1, where a user of interest u_i is positioned in the internal circumference of radius $d = 50$ m, while the other (interfering) users u_j are located in the external circumference of radius d_{interf}, with both of the circumferences centred at the BS. To obtain different levels of MAI, we combine different numbers of active users (K) with different external radius values d_{interf}, as well as the average channel condition of the interest and interfering users. In this sense, let us define the coupling network parameter:

$$\beta_k = \frac{\langle \mathrm{h}_k \rangle}{\langle \mathrm{h}_j \rangle}, \quad k : \text{interest user}; \; j \neq k : \text{interfering users}$$

where $\langle \cdot \rangle$ is the temporal average operator. With the proposed topology, we can create scenarios with increasing interference level: increasing the system loading as well as reducing the distance between interfering users and the BS, which implies higher β_k. Hence, the max-EE and the opt-SE behaviour were characterised in terms of $d_{\mathrm{interf}}^{-\iota}$, $\iota \geq 2$.

Figure 2 and Table I presents the EE–SE trade-off for different system configurations, considering $K = [3, 6, 9]$ users, $d_{\mathrm{interf}} = [200, 100, 80]$ m and $N = 15$. In Figure 2, the curves with markers '+' refer to the right-hand side y-axis, that is, the allocated power (proportional to the achieved SINR) versus SE (bits per second/Hertz), while the curves without markers refer to the left-hand side y-axis, relating the EE in bits per Joule versus the achieved SE. Plots (a), (b) and (c) of Figure 2 refer to the results obtained with MF detector, while plot (d) depicts the simulation results obtained with DEC multi-user detector, which carried on the same curves for all d_{interf} values in the considered range of [80; 200] m. Table II highlights notable values found in Figure 2, such as the maximal achievable SE and its respective utility function.

Trans. Emerging Tel. Tech. **26**:670–685 (2015) © 2013 John Wiley & Sons, Ltd.
DOI: 10.1002/ett

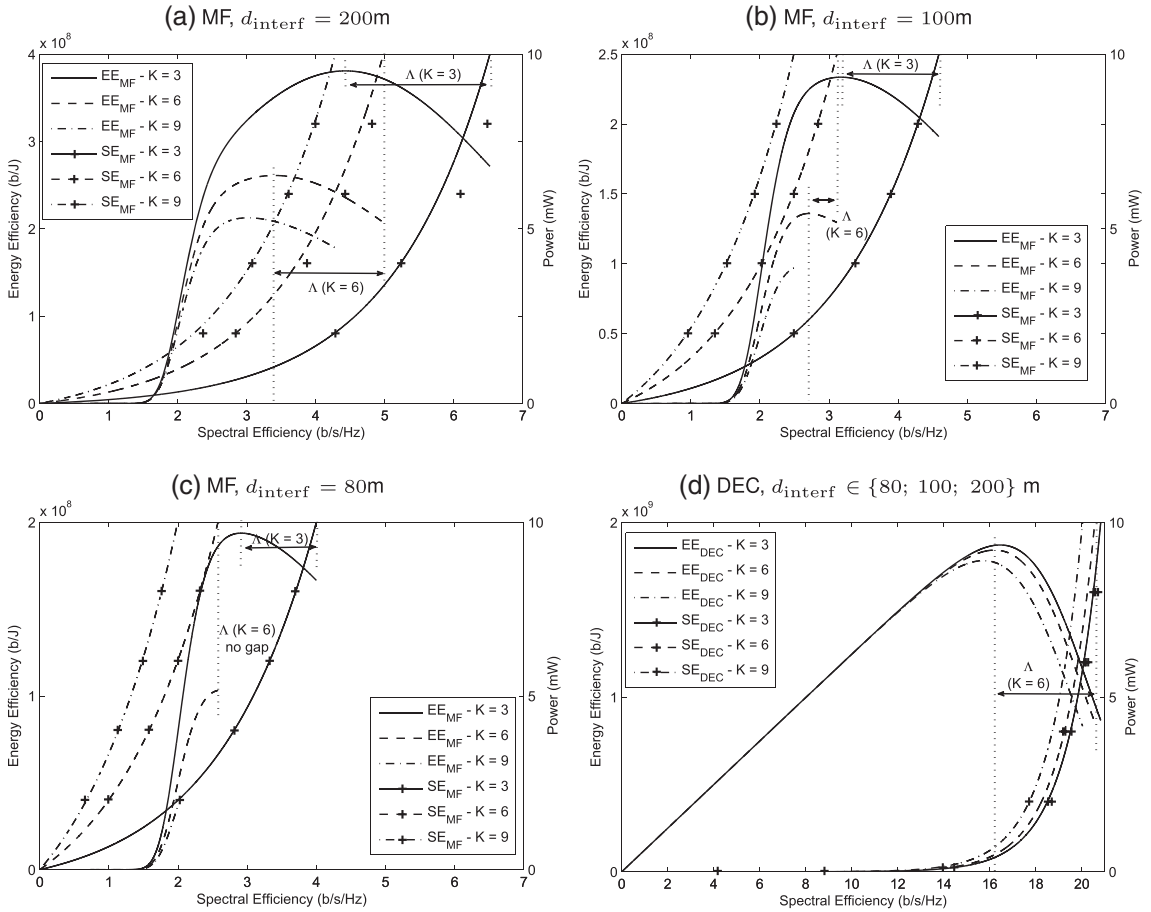

Figure 2. Energy efficiency–spectral efficiency (EE–SE) trade-off considering different interfering scenarios and filters: (a) matched filter (MF), $d_{\mathrm{interf}} = 200$ m, $\beta_k = 0.25$; (b) MF, $d_{\mathrm{interf}} = 100$ m, $\beta_k = 0.50$; (c) MF, $d_{\mathrm{interf}} = 80$ m, $\beta_k = 0.63$; (d) decorrelator (DEC), $d_{\mathrm{interf}} \in$ [80; 200] m.

Table I. Notable values for the results of Figure 2: SE at maximum EE and its respective utility function value; maximal achievable SE and its respective utility function value; and the SE gap Λ.

Scenario	$\zeta(\gamma_k^{\mathrm{EE}})$ [b/s/Hz]		$u_k(\gamma_k^{\mathrm{EE}})$ [b/J]		$\zeta(\gamma_k^{\mathrm{SE}})$ [b/s/Hz]		$u_k(\gamma_k^{\mathrm{EE}})$ [b/J]		Λ [b/s/Hz]	
(a) $K = 3$	MF	DEC	MF	DEC	MF	DEC	MF	DEC	MF	DEC
$d_{\mathrm{int}} = 200$ m	4.4302	16.4198	$3.8087 \cdot 10^8$	$1.8676 \cdot 10^9$	6.5244	20.7916	$2.7163 \cdot 10^8$	$8.6563 \cdot 10^8$	2.0942	4.3718
$d_{\mathrm{int}} = 100$ m	3.1704	16.4317	$2.3355 \cdot 10^8$	$1.8693 \cdot 10^9$	4.5891	20.8065	$1.9106 \cdot 10^8$	$8.6625 \cdot 10^8$	1.4187	4.3748
$d_{\mathrm{int}} = 80$ m	2.9139	16.4508	$1.9374 \cdot 10^8$	$1.8715 \cdot 10^9$	4.0008	20.8256	$1.6657 \cdot 10^8$	$8.6705 \cdot 10^8$	1.0869	4.3748
(b) $K = 6$	MF	DEC	MF	DEC	MF	DEC	MF	DEC	MF	DEC
$d_{\mathrm{int}} = 200$ m	3.4017	16.1843	$2.6112 \cdot 10^8$	$1.8382 \cdot 10^9$	4.9805	20.5324	$2.0736 \cdot 10^8$	$8.5484 \cdot 10^8$	1.5788	4.3481
$d_{\mathrm{int}} = 100$ m	2.7083	16.1963	$1.3597 \cdot 10^8$	$1.8399 \cdot 10^9$	3.1130	20.5473	$1.2952 \cdot 10^8$	$8.5546 \cdot 10^8$	0.4047	4.3510
$d_{\mathrm{int}} = 80$ m	2.5777	16.2154	$1.0320 \cdot 10^8$	$1.8420 \cdot 10^9$	2.5777	20.5664	$1.0320 \cdot 10^8$	$8.5626 \cdot 10^8$	0	4.3510
(c) $K = 9$	MF	DEC	MF	DEC	MF	DEC	MF	DEC	MF	DEC
$d_{\mathrm{int}} = 200$ m	3.0203	15.7009	$2.1261 \cdot 10^8$	$1.7781 \cdot 10^9$	4.2823	20.0027	$1.7829 \cdot 10^8$	$8.3279 \cdot 10^8$	1.2620	4.3018
$d_{\mathrm{int}} = 100$ m	2.4889	15.7158	$9.6933 \cdot 10^7$	$1.7798 \cdot 10^9$	2.4889	20.0176	$9.6933 \cdot 10^7$	$8.3341 \cdot 10^8$	0	4.3018
$d_{\mathrm{int}} = 80$ m	1.9951	15.7320	$3.6446 \cdot 10^7$	$1.7819 \cdot 10^9$	1.9951	20.0367	$3.6446 \cdot 10^7$	$8.3420 \cdot 10^8$	0	4.3047

SE, spectral efficiency; EE, energy efficiency; MF, matched filter; DEC, decorrelator.

Table II. EE–SE trade-off analysis.

Parameters	Adopted values
DS/CDMA optimal power allocation	
Noise Power	$P_n = -90$ dBm
Processing Gain	$N = 15$
Maximum power per user	$P_{max} = 10$ dBm
No. of mobile terminals	$K \in \{2; 10\}$
No. of base station	BS = 1
Interest user distance	$d = 50$ m
Interfering users distance	$d_{interf} = [80, 100, 200]$ m
Packet size	$M = 80$ bits
Data bits	$L = 50$ bits
SINR gap	$\theta_k = 0.651$
Circuit power	$p_c = 7$ dBm
Bandwidth	$\mathtt{w} = 10^6$ Hz
Channel gain	
Path loss	$\propto d^{-2}$
Fading coefficients	Rayleigh distribution mean over 5000 realisations
Verhulst PCA	
Convergence factor	$\alpha = 0.5$
No. of iterations	$N_{it} = 500$

EE, energy efficiency; SE, spectral efficiency; DS/CDMA, direct sequence code division multiple access; SINR, signal-to-interference-plus-noise ratio; PCA, power control algorithm.

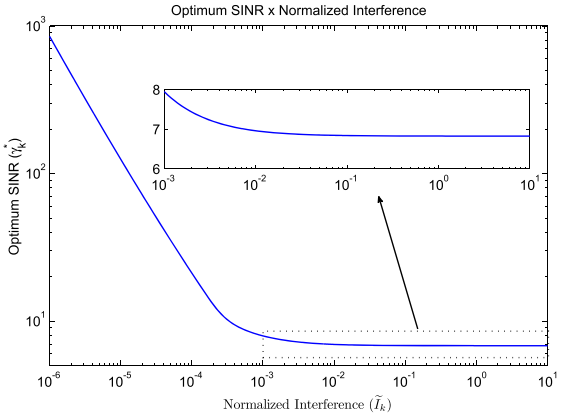

Figure 3. Optimum energy efficiency signal-to-interference-plus-noise ratio (SINR) versus normalised interference. $M = 80$ and $\theta = 0.651$.

As can be seen from Figure 2(a), (b) and (c) under MF SuD, gap Λ and the EE are severely reduced when the system loading increases and the interfering users distance d_{interf} decreases. For example, when $d_{\text{interf}} = 200$ m, the EE is almost halved for the interest user when the number of active users is increased from $K = 3$ to $K = 9$. Likewise, when $K = 6$, the EE is also halved when the interfering users distance is reduced from $d_{\text{interf}} = 200$ m to $d_{\text{interf}} = 100$ m. In terms of gap Λ, when the MAI increases, Λ is reduced, tending to be zero for higher system loadings and lower interfering users distance, as pointed out for $K = 6$ in Figure 2 (a)–(c), when d_{interf} decreases from 200 to 80 m, respectively.

Furthermore, in order to corroborate those conclusions and to determine the impact of the MAI on the EE problem, we analyse the impact of linear multi-user filter deployment, represented by DEC multi-user detector. We analysed the performance under the same system scenario adopted with the MF single-user detector, and surprisingly, we found approximately the same gap Λ and EE for DEC, as can be concluded from Table I and Figure 2(d). Now, comparing the EE and SE performance from Figure 2(a)–(c), with Figure 2(d), both EE and SE are seen to be degraded with the MF detector when the system loading increases and d_{interf} decreases. Considering the best and worst cases of K and d_{interf}, while the MF-based system is reduced by a factor of 10 from $K = 3$ and $d_{\text{interf}} = 200$ m to $K = 9$ and $d_{\text{interf}} = 80$ m, the EE for DEC is almost the same for both configurations. Also, the EE is at least 4.9 times greater for DEC when compared with that obtained with MF. Finally, as the SINR achieved with DEC filter, Equation (5), does not depend on the power level of interfering users, the EE is almost the same for any interfering users position, which is corroborated by our simulations.

4.1. Circuit power consumption, multiple access interference and optimum signal-to-interference-plus-noise ratio

When the circuit power consumption is much smaller than the transmitted power ($p_c \ll p_k$), an interesting result is derived: the optimum SINR obtained from the EE optimisation problem in Equation (20) is the same for any MAI level, while the asymptotic SINR necessary to the SE maximisation still remains related to the interference power level, $\widetilde{I}_k$. Hence, under this hypothesis, the best SINR for max-EE criterion depends only on the system parameters, such as maximal tolerable BER (QoS), modulation level, coding and packet coding size. This result is well known in the literature, as can be seen in [7, 8]. Besides, it is worth noting that when the MAI increases, the transmitted power per user becomes higher, and indeed, the condition $p_c \ll p_k$ holds.

In order to verify the impact of the normalised MAI $\widetilde{I}_k$ on the optimum SINR γ_k^*, that is, the SINR at the maximal EE point equilibrium, Figure 3 shows the γ_k^* for a wide range of $\widetilde{I}_k$, revealing that when system interference is low, the p_c term at the denominator of Equation (11) allows the system to use more power to transmit, because $\gamma_k \widetilde{I}_k$ tends to be lower than p_c. When $\widetilde{I}_k$ becomes greater, we have the condition $p_k \gg p_c$, and optimum SINR tends to converge.

Trans. Emerging Tel. Tech. **26**:670–685 (2015)
DOI: 10.1002/ett

As concluded from the results, when the MAI increases, Λ is drastically reduced for MF. This shows that the best EE–SE trade-off is to allocate the necessary power to achieve the maximum EE. In the case of the DEC detector, our simulations indicated that Λ remains almost the same with increasing system loading, indicating that multi-objective optimisation techniques are necessary to determine the best EE–SE trade-off. This investigation is also left for future work.

Because we defined the best EE–SE trade-off, in the next section, two iterative-approximative algorithms will be suggested in order to implement/verify the conclusions found earlier.

5. PROPOSED ENERGY EFFICIENCY–SPECTRAL EFFICIENCY ALGORITHMS

As described in the previous section, MAI plays a key role in the EE performance; this way, reducing MAI is critical to obtain higher EE. Looking at the EE maximisation problem described in Equation (17) and the strict quasi-concavity of ξ_k, when $p_k^* > P_{\max}$, we have that ξ_k is strictly increasing in the interval $[0, P_{\max}]$, and the kth user selfishly allocates the maximum available power. This behaviour tends to increase the MAI power level for all users, reducing the EE. As demonstrated in [3], the ratio of users transmitting at $P_{\max}$ can be approximately 80 per cent in full system loading.

The algorithm proposed to implement the optimal EE–SE trade-off solution is described in Algorithm 1. The MAI is determined via SINR measurement, and the optimum SINR is obtained by solving Equation (20), that is, the SINR of maximum EE; after that, the optimum power for each mobile user is found by iteratively applying Verhulst-based PCA [26]. If one or more users cannot achieve the optimum EE, given the maximum power constraint, then they are put in outage. The set of users in outage is given by K_{out}.

In order to minimise the outage probability, an alternative approach is proposed in Algorithm 2. Instead of putting all users that cannot achieve optimum EE in outage, Algorithm 2 considers the QoS metrics for each user in the decision process. As we defined the minimum data rate $R_{k,\min}$ as a QoS metric, if one user cannot achieve the optimum EE but is able to maintain $R_{k,\min}$, then this user is not put in outage; however, if both optimum EE and $R_{k,\min}$ are not obtained, the outage event occurs.

The evaluation of $\widetilde{I}_k$ is made with BS information; transmitted by a feedback channel, the BS communicates to all the users the SINR achieved between themselves and the BS. Because all users know their own transmitted power, they just need to divide the communicated SINR by the power allocated, obtaining $\widetilde{I}_k$.

Algorithms 1 and 2 are closely related. It is easy to see that when the necessary SINR $\gamma_{k,\min}$ to achieve $R_{k,\min}$ is greater than or equal the optimum SINR (γ_k^*), Algorithm 2 reduces to Algorithm 1, because the second condition to be inserted in K_{out} is always true for all non-optimum users. Besides, if we set $R_{k,\min} = 0$, Algorithm 2 will have the same behaviour as the problem defined in Equation (17), equivalent to the classic approach in the literature.

Algorithm 1 EE–SE with optimum EE

Require: $i \leftarrow 1$, N_{it}, $p_k[0] = \sigma_k^2\ \forall k$
  while $i \leqslant N_{it}$ **do**
    for $k = 1 : K$ **do**
      Evaluate $\widetilde{I}_k$ (via SINR_k measurement);
      Find γ_k^*, by solving Equation (20);
      Find p_k^* iteratively using Verhulst PCA [26];
    end for
    $i = i + 1$;
  end while
  Compute the SINR achieved (γ_k) for each user;
  Compute K_{out}, where $k \in K_{\text{out}}$ if $\gamma_k < \gamma_k^*$;
  if $\{K_{\text{out}}\} \neq \emptyset$ **then**
    Find the user with the worst channel gain in K_{out} (jth user);
    Set $\gamma_j^* = 0$;
    Go to the beginning;
  else
    return $p_k^*\ \forall k$;
  end if

Algorithm 2 EE–SE with $R_{k,\min}$ criterion

Require: $i \leftarrow 1$, N_{it}, $p_k[0] = \sigma_k^2\ \forall k$
  Compute p_k^* as described in Algorithm 1;
  Compute the SINR (γ_k) and rate (r_k) achieved for each user;
  Compute K_{out}, where $k \in K_{\text{out}}$ if $\gamma_k < \gamma_k^*$ and $r_k < R_{k,min}$
  if $\{K_{\text{out}}\} \neq \emptyset$ **then**
    choose the user with worst channel gain in K_{out} (jth user)
    set $\gamma_j^* = 0$;
    go to the beginning.
  else
    return $p_k^*\ \forall k$ (EE–SE trade-off solution)
  end if

After defining the algorithms, we need to investigate the existence and uniqueness of the equilibriums achieved. Defining the equilibrium point by $\mathbf{p}^* = (p_1^*, p_2^*, \cdots, p_k^*)$, the Nash equilibrium can be defined as follows.

Definition 2 (Nash equilibrium)**.** *An equilibrium is said to be a Nash equilibrium if and only if any user cannot unilaterally improve its response by changing the optimum value* [15]. *In the context of the EE problem, this statement is equivalent to the fact that no user can improve their*

utility value by changing the optimum power for any other value:

$$u_k\left(p_k^*, \mathbf{p}_{-k}^*\right) \geq u_k\left(p_k, \mathbf{p}_{-k}^*\right), \quad \forall k \tag{24}$$

Because the two algorithms proposed do not necessarily result in the same equilibrium $\mathbf{p}^*$, we must discuss the equilibria achieved by Algorithms 1 and 2. However, because the existence of the Nash equilibrium depends on the game (the utility function), we first prove that the proposed game has the minimum properties that guarantee the existence of the Nash equilibrium, resulting in the following theorem.

Theorem 1. *The system achieves at least one equilibrium* $\mathbf{p}^*$ *for both algorithms, and each* $p_k^* \in \mathbf{p}^*$ *is defined by the following conditions for Algorithm 1*

(1) If $p_k \leq P_{\max}$ *and* $\frac{\partial(u_k(p_k, \mathbf{p}_{-k}^*))}{\partial p_k} = 0$, *then* $p_k^* = p_k$
(2) Else, $p_k^* = 0$

and for Algorithm 2

(1) If $p_k \leq P_{\max}$ *and* $\frac{\partial(u_k(p_k, \mathbf{p}_{-k}^*))}{\partial p_k} = 0$, *then* $p_k^* = p_k$
(2) If $p_k = P_{\max}$, $\frac{\partial(u_k(p_k, \mathbf{p}_{-k}^*))}{\partial p_k} \neq 0$ *and* $r_k \geq R_{k,min}$, *then* $p_k^* = P_{\max}$
(3) Else, $p_k^* = 0$

Proof. See the Appendix. □

The first condition in Theorem 1 for Algorithm 1 occurs when the user has sufficient power to achieve the optimum SINR point, and the second condition occurs when the user cannot achieve the optimum point, that is, the outage scenario.

Similarly, the first condition in Theorem 1 for Algorithm 2 corresponds to the case when the kth user achieves optimum EE setting his power to less than or equal to the maximum power available at the transmitter. The difference is for the situation in which the user cannot achieve the maximum efficiency but achieves a minimum rate criterion, defined in the second case, setting his transmit power to the maximum power available. Finally, when the two criteria fail, the user must set his transmit power to zero, as in the second case for Algorithm 1.

The uniqueness and Pareto optimality of the Nash equilibrium for this non-cooperative game is summarised in Lemma 2. The proof for this lemma is developed in the Appendix.

Lemma 2. *When equilibrium* $\boldsymbol{p}^*$ *is achieved without removing any user, this Nash equilibrium is unique. When it is necessary to remove any user, multiple equilibriums will exist, depending on the criterion adopted. For the criterion we adopted, the equilibrium is also unique. About Pareto optimality, the equilibrium obtained with MF detector is not Pareto optimal, while that obtained with DEC is Pareto optimal* [9].

6. NUMERICAL RESULTS

The system parameters are indicated previously in Table II. In particular, the analysis in this section assumes a ring geometry, with internal radius $r_{\text{int}} = 50$ m and external radius $r_{\text{ext}} = 200$ m, with K mobile users uniformly distributed in this ring area with radius$\sim \mathcal{U}[r_{\text{int}}, r_{\text{ext}}]$, and the BS in the centre of the ring. The processing gain was assumed $N = 63$; the number of MTs was $K \in \{2; 15\}$ (low system loading) for the first set of results and $K \in \{3; 63\}$ for the second set (from low to full system loading). For simplicity, identical parameters of QoS were adopted for all users, that is, SINR gap $\theta_k = 0.651$, and minimum data rate $R_{\min} = 500$ kbps. Fading is modelled as a non-selective Rayleigh distribution (module), simulated as a complex Gaussian random process, with zero mean and variance given by $\sigma^2 = d_k^{-2}$, namely $h_k \sim \mathcal{CN}(0, d_k^{-2})$, where d_k is the distance between kth user and the BS. In order to analyse the average network behaviour, numerical results were taken as the average over 2000 network realisations. Furthermore, it was assumed that the mobile transmitter has perfect channel state information available, but the measurement of other users channel state information can only be carried out by the BS through quantised transmitted bits. For Verhulst PCA, a convergence factor $\alpha = 0.5$ and number of iterations $N_{it} = 500$ were assumed.

Figures 4–7 bring the four main metric figures in order to analyse and to quantify performance gain of the two algorithms proposed against the classical approach defined in Equation (17), that is, (i) the attainable sum rates of all users, $\sum R$; (ii) the sum of power level consumption, including the circuit power, $\sum P$; (iii) the overall EE, obtained from the two algorithms for the two detectors considered; and finally, (iv) the percentage of users in outage is calculated.

From Figure 4, one can conclude that the classical approach described by Equation (17) achieves the best result in terms of sum rate maximisation, mainly when the system loading increased under conventional receiver, followed by Algorithms 2 and 1. It is worth pointing out that under the multi-user DEC filter, the $\sum R$ differences for all algorithms are negligible, and the cause is the null outage probability for DEC, as will be further discussed in Figure 7. Besides, because under the classical approach, no user was put in outage, all of them contribute to increase the $\sum R$, even by transmitting with a little rate. For Algorithm 1, the higher outage probability limits the $\sum R$, and for Algorithm 2, the lower outage probability keeps its $\sum R$ between the two other algorithms.

For sum power metric (Figure 5), the non-outage behaviour described by Equation (17) implies higher power consumption for the MF, because non-optimum users

Trans. Emerging Tel. Tech. **26**:670–685 (2015)
DOI: 10.1002/ett

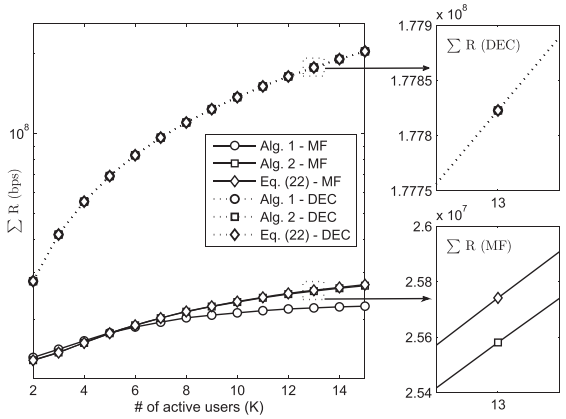

Figure 4. Sum rate ($\sum R$) for the two algorithms proposed and two different filters. In detail, the $\sum R$ is for the decorrelator (DEC) and $\sum R$ for the matched filter at $K = 13$ users, emphasising the gap among both algorithms proposed.

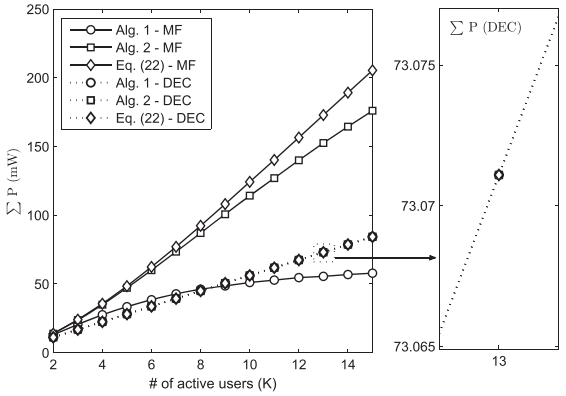

Figure 5. Sum power ($\sum P$) for the two algorithms proposed and two different filters. In detail, the $\sum P$ is achieved by the decorrelator (DEC) at $K = 13$, emphasising the null performance gap among both algorithms proposed for low system loading. MF, matched filter.

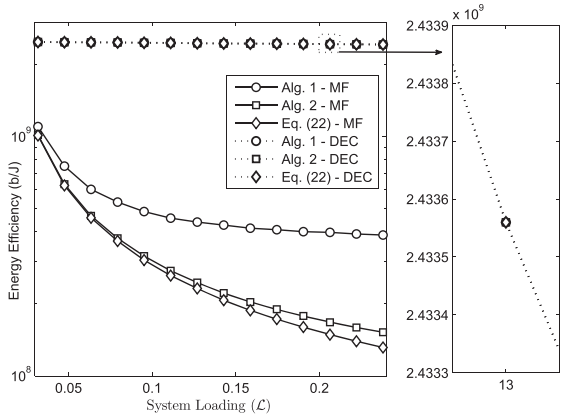

Figure 6. Energy efficiency for the two algorithms proposed and detectors. DEC, decorrelator; MF, matched filter.

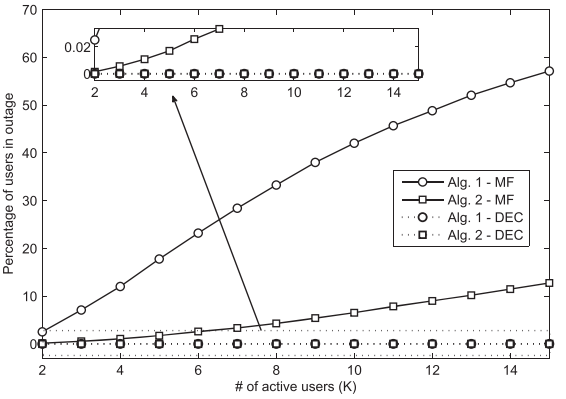

Figure 7. Percentage of users in outage for the two algorithms proposed. Herein, the adopted processing gain is $N = 63$. DEC, decorrelator; MF, matched filter.

transmit at maximum power. As some users are put in outage, Algorithm 2 reduces the $\sum P$ but keeps some non-optimum because the minimum rate criteria was reached. For Algorithm 1, all non-optimal users will be in outage state, and then, the $\sum P$ is minimised. Again, because no outage occurs for all algorithms for DEC, no gaps can be seen. Because the DEC is more efficient than the MF for MAI mitigation, the system is able to support more users under DEC multi-user filter.

Figure 6 indicates the EE behaviour against increasing system loading (when the number of active users increases). When $K \geqslant 7$, despite the sum rate improvement obtained by Algorithm 2 and the problem described in Equation (17) over Algorithm 1 considering the MF detector, this improvement is obtained at the system's EE degradation cost (Figure 6). This behaviour is justified by the fact that there are users transmitting with non-optimal powers in Algorithm 2 and Equation (17). Besides, the best response in terms of EE is achieved by Algorithm 1 but incurs in more users in outage. As pointed out before, the multi-user DEC detector is more efficient than the MF for the two algorithms proposed, thanks to its improved capacity to provide MAI mitigation.

Despite the null difference in sum rate (or sum power) performance between the two algorithms proposed operating under DEC filter, both algorithms proposed present remarkable efficiency increase, because the rate achieved is higher and simultaneously the allocated power is smaller than that attainable with MF.

Figure 7 shows the impact of the MAI on receivers equipped with matched and DEC filter-based systems. System loading was confined in the interval $K/N \in [0.0317; 0.2381]$. Hence, even under low system loading, Algorithm 1-based system is not able to achieve the maximum EE point for all users using MF, because the power required to achieve the optimum SINR increases as the interference increases, and then, the maximum power available is overcome very soon. On the other hand, because Algorithm 2 allows users to transmit over a non-optimum power level scenario (as long as the minimum

rate criterion is reached), the outage probability will be smaller. Again, thanks to the MAI mitigation characteristics of the DEC filter, no outage events were detected for low system loading.

It is worth noting that the performance gaps among the two algorithms proposed—mainly deployed with MF-based systems—can be explained by the numerical value for the minimum rate adopted, which requires low SE ($\eta_k = 0.5$) to be achieved, while allowing a better visualisation of the performance difference. By adopting a higher value for the minimum rate, the expectation is that the outage probability will be increased for the two filters (MF and DEC), while the performance difference among Algorithms 1 and 2 will be decreased.

Finally, in order to corroborate the DEC efficiency and the MAI mitigation impact on the system performance, the same metrics were then analysed, considering only the DEC performance with $K \in \{3; 63\}$ (i.e. low to high loading system conditions). To demonstrate the impact of the minimum rate criteria and the fact that the results of Algorithm 2 are constrained by Algorithm 1 and the problem defined in Equation (17), we use two minimum rate values: $R_{k,\min} = 50$ kbps and $R_{k,\min} = 1$ Mbps. Those metrics are illustrated in Figures 8–11.

Figures 8 and 9 show the sum rate and the sum power for the two algorithms proposed deploying multi-user DEC filter; again, Algorithm 1 presents the best response in terms of power minimisation. The remarkable difference gain occurs in the higher system loading zone. Furthermore, with Algorithm 1 running, a higher sum rate regarding Algorithm 2 and Equation (17) is attained, because the DEC filter depends on the spreading codes correlation (pseudo-noise sequences are adopted). Thus, under high system loading condition (above $K = 54$ users), the average MAI (given by the average of $\mathcal{I}_k$ of the denominator in Equation (5)) becomes higher and limits the achievable SINR. Because Algorithm 1 is more susceptible to outage

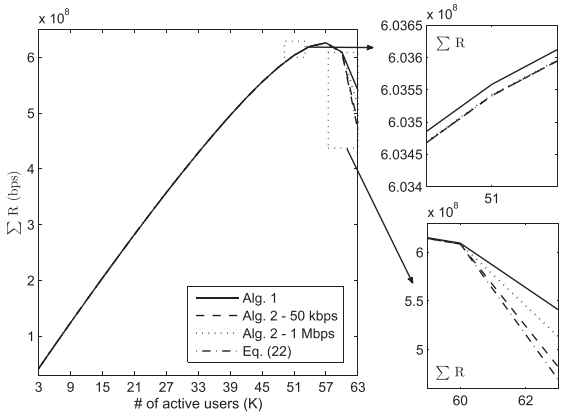

Figure 8. Sum rate ($\sum R$) for the two algorithms proposed and the decorrelator (DEC) filter. In detail, the $\sum P$ and $\sum R$ are achieved by the DEC at $K = 14$, emphasising the small performance gap in both algorithms proposed.

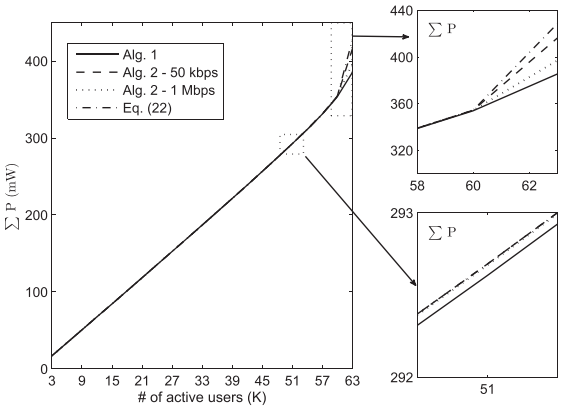

Figure 9. Sum power ($\sum P$) for the two algorithms proposed and the decorrelator (DEC) filter. In detail, the $\sum P$ and $\sum R$ are achieved by the DEC at $K = 14$, emphasising the small performance gap among both algorithms proposed.

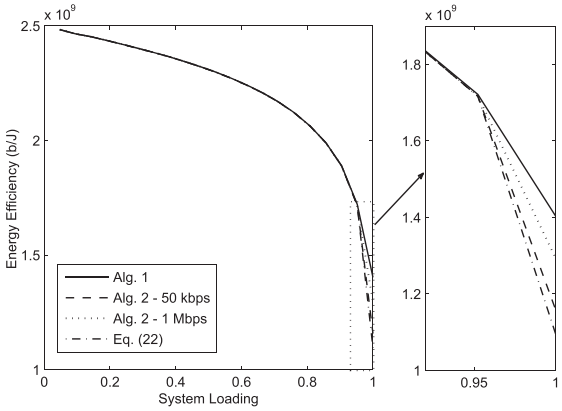

Figure 10. Energy efficiency for the two algorithms proposed for the decorrelator.

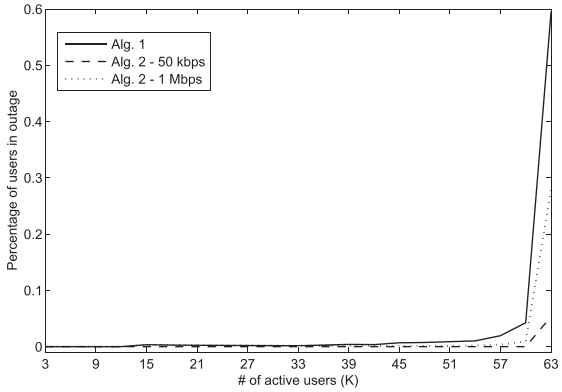

Figure 11. Percentage of users in outage for the two proposed algorithms deploying the decorrelator filter; $N = 63$.

Trans. Emerging Tel. Tech. **26**:670–685 (2015) © 2013 John Wiley & Sons, Ltd.
DOI: 10.1002/ett

than the other algorithms (Figure 11), those removed users reduce the noise enhancement, and other users can achieve greater SINR values. When using $R_{k,\min} = 1$ Mbps, Algorithm 2 results are closer to the performance of Algorithm 1, and when $R_{k,\min} = 50$ kbps, the results are closer to the problem in Equation (17).

In terms of EE, given by Figure 10, both algorithms proposed present slightly decreasing EE with system loading increasing, but this decrease becomes more prominent when the system loading approaches 1, in which the EE difference among both algorithms increases substantially, mainly when $\mathcal{L} = K/N \geqslant 90$ per cent. Under medium and low system loadings, there are no noticeable differences in EE, as shown in Figure 6. In conclusion, as expected, Algorithm 1 is the most energy efficient, and even under full system loading ($\mathcal{L} = 1$), the DEC filter is more efficient than MF-based systems for low and medium loadings, whatever algorithm is deployed. Both algorithms are more energy efficient than the problem defined in Equation (17).

Finally, in Figure 11, the percentage of users in outage for both algorithms with DEC filter can be examined. Under medium and mainly high system loading, the EE-efficient system equipped with DEC filter achieves much lower user outage probability than with MF-based systems (when comparing the same algorithms), even with a loading four times higher. For example, while the MF-based system equipped with Algorithm 1 presents an average of 8.56 users in outage of 15 active users, the same system based on the DEC filter is able to reduce the average users in outage to only 0.375 users removed of 63 active users. For Algorithm 2, while the MF-based has an average of 1.91 users removed every 15 active users, with the DEC filter, the algorithm removes only 0.01755 of 63 active users. These results demonstrate the impact of MAI in the equilibrium and the ability of the multi-user DEC filter to mitigate MAI. In conclusion, Algorithm 1 is less efficient in terms of outage probability than Algorithm 2.

7. CONCLUSIONS

In this work, we analysed the EE and SE in the multiple access DS/CDMA systems. The distributed EE cost function is elaborated from the perspective of the two conflicting metrics, throughput maximisation and power level consumption minimisation, as well as the impact of multi-user filter deployment over the EE–SE trade-off.

We found that SINR under the max-EE point equilibrium decreases when MAI power level increases, being, however, almost the same under medium or high interference scenarios. For MF, the best EE–SE trade-off consists in allocating in each node the necessary transmit power to achieve the maximal EE, while SE can be determined by the attainable rate in each node given by the Shannon capacity equation.

Employing different figures of merit, numerical results indicated that by deploying both power allocation algorithms proposed, the linear multi-user filter is much more efficient than the conventional MF receiver.

Finally, because the DEC detector is more efficient in providing MAI mitigation, a new formulation for the max-EE *versus* opt-SE trade-off problem, considering multi-objective techniques, would be proposed as a new research direction in the field.

APPENDIX

Proof of strict quasiconcavity of the utility function

Proof. In order to prove that our utility function is strictly quasiconcave, first we demonstrate that the numerator of the utility function, that is, $(1 - e^{-\gamma})^M \log_2(1 + \theta\gamma)$, is S-shaped. As described in [25], if our utility function is $f(x)/x$ and $f(x)$ is S-shaped, then we can guarantee that $f(x)/x$ is strictly quasiconcave. According to [25], there are six conditions that need to be proven to state that a function is S-shaped:

- C1 Function domain ($\mathbf{X}$) is the non-negative part of the real line, $[0, \infty)$;
- C2 The range is the interval $[0,\ B)$, generally with $B = 1$;
- C3 It is increasing;
- C4 The first derivative is continuous.
- C5 Strictly convex in the interval $[0, x_i], x_i \in \mathbf{X}$;
- C6 Strictly concave in the interval $[x_i, L], L > x_i$;

Condition C1 is obvious, because $\gamma_k \geqslant 0$.

At first, C2 appears to be false, because $\lim_{\gamma_k \to \infty} = \infty$, but because our scenario includes power limitation, it is obvious that $\lim_{\gamma \to \gamma_{\max}} = b$, where $b \in \mathbb{R}$ and $\gamma_{\max}$ is the maximum achievable SINR.

Condition C3 is also obvious, because

$$(1 - e^{-\gamma_i})^M > (1 - e^{-\gamma_j})^M \,\forall\, \gamma_i > \gamma_j$$

and

$$\log_2(1 + \theta\gamma_i) > \log_2(1 + \theta\gamma_j), \forall\ \gamma_i > \gamma_j .$$

Condition C4 is also true, because the first derivative of $(1 - e^{-\gamma})^M \log_2(1 + \theta\gamma)$, given in Equation (25), has a unique restriction to the continuity $(1 + \theta\gamma > 0)$. Because $0 < \theta < 1$ and $\gamma \geqslant 0$, $(1 + \theta\gamma) \geqslant 1$.

$$\frac{\partial\{(1 - e^{-\gamma})^M \log_2(1 + \theta\gamma)\}}{\partial\gamma} = \frac{(1 - e^{-\gamma})^M \theta}{(1 + \theta\gamma)\ln(2)} + Me^{-\gamma}(1 - e^{-\gamma})^{(M-1)} \log_2(1 + \theta\gamma) \quad (25)$$

As conditions C5 and C6 are hard to demonstrate, we use numerical evidences to confirm them. The strict convexity of a given function can be confirmed looking at the first

derivative: if $f(x)$ is strictly convex and $f'(x)$ is continuous, then $f'(x)$ is increasing. Likewise, the strict concavity can be analysed by the first derivative: if $f(x)$ is strictly concave and $f'(x)$ is continuous, then $f'(x)$ is decreasing. Thus, if the numerator is S-shaped, it is obvious that there is a unique inflection point at the first derivative of the EE numerator, that is, at the point the first derivative stops increasing and starts to decrease. In order to determine this point, we take the second derivative of the numerator regarding γ_k, and equate it to zero, obtaining

$$\frac{2\theta e^{-\gamma} M(1-e^{-\gamma})}{(1+\theta\gamma)} - \frac{\theta^2(1-e^{-\gamma})^2}{(1+\theta\gamma)^2} - Me^{-\gamma}\log(1+\theta\gamma) + M^2 e^{-2\gamma}\log(1+\theta\gamma) = 0 \quad (26)$$

Determining an explicit function to calculate the inflection SINR, γ_{infl}, which is the solution of Equation (26), for any value of M and θ, becomes an extremely hard task. Hence, in order to show the existence of γ_{infl}, we plot the first derivative of EE numerator for a wide range of combinations of M and θ, as shown in Figure A.1. Because a 4D plot would be required to visualise the solution for all possible combinations, firstly we consider a fixed value for M with $0.15 \leqslant \theta \leqslant 0.99$, and then, we range M from 2 to 100 with fixed θ. These plots show that there is at least one inflection point and that the packet size impact is much more prominent than gap factor θ.

Hence, verifying the first derivative of the EE numerator for a wide range of combinations of M and θ, the inflection point is verified to exist. To determine the inflection SINR, we used the *fzero* tool from MATLAB® (Release 2010a, The MathWorks, Inc., Natick, Massachusetts, United States) and analysed the range $0.15 \leqslant \theta \leqslant 0.99$ and $2 \leqslant M \leqslant 100$. From Figure A.2, one can see that the inflection point increases when M increases and θ decreases, as expected from the numerical evidences of Figure A.1.

Under these numerical evidences, we state that the numerator of the EE utility function is S-shaped, and, as a consequence, the statement of Rodriguez [25, Sec. IV] can be invoked to prove that the utility function in Equation (17) is strictly quasiconcave; Lemma 1 thus holds. □

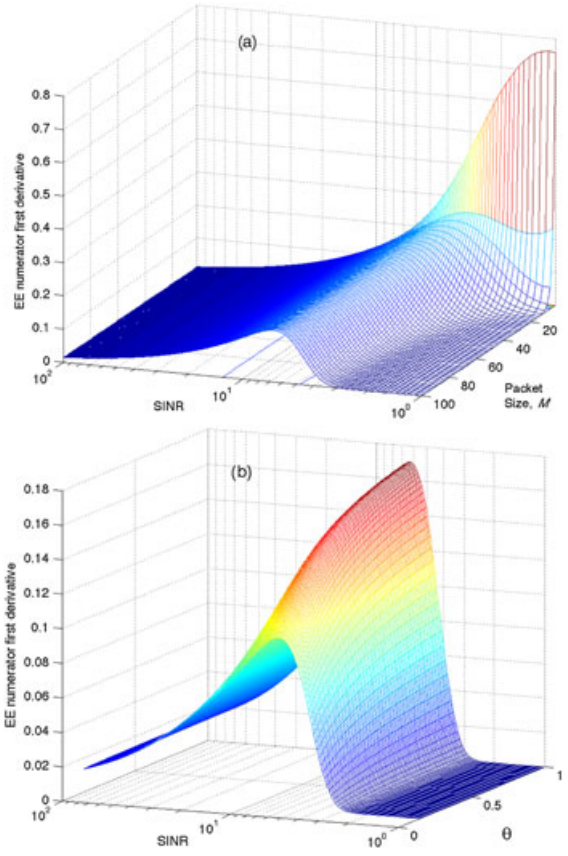

Figure A.1. First derivative from the numerator of the utility function, discarding the constant factor L/M, for: (a) different values of M and fixed $\theta = 0.651$; (b) different values of θ and fixed $M = 80$. EE, energy efficiency; SINR, signal-to-interference-plus-noise ratio.

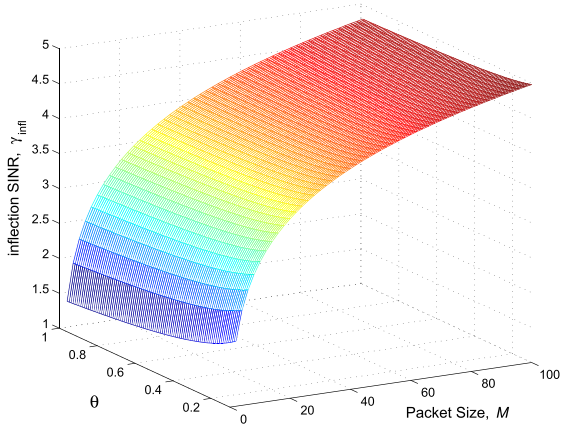

Figure A.2. Inflexion signal-to-interference-plus-noise ratio (SINR) (solution of Equation (26)) for different values of M and θ.

Proof of Theorem 1

Proof. The proof presented is similar to that discussed in [27]. As pointed out herein, there are three conditions to confirm the existence of the Nash Equilibrium:

- C1 Strategy set $\mathcal{A}_k$ is a non-empty, convex and compact subset of some Euclidian space;
- C2 The utility function for the kth user $(u_k(p_k, \mathbf{p}_{-k}))$ is continuous for all $\mathbf{p}_{-k}$ and $p_k \in \mathcal{A}_k$; item[C3] The utility function for the kth user $(u_k(p_k, \mathbf{p}_{-k}))$ is quasiconcave in p_k (or γ_k);

Trans. Emerging Tel. Tech. **26**:670–685 (2015)
DOI: 10.1002/ett

Condition C3 was proven in the first section of this Appendix.

Condition C2 can be proven by looking at the definition of u_k, $u_k(\gamma_k) = \frac{\ell_k w \log_2(1+\gamma_k\theta_k)(1-e^{\gamma})^M}{\gamma_k \widetilde{I}_k + p_c}$. The first condition to the continuity of u_k is that the denominator is different from zero, $\gamma_k \widetilde{I}_k + p_c \neq 0$. Because interference is non-negative for both filters for any $\mathbf{p}_{-k}$ (Equation (18)) and p_c is positive, we have that the denominator never equals zero. The second condition is that $1 + \gamma_k\theta_k > 0$, because the logarithm operation is not defined for non-positive arguments. Because $\gamma_k \geqslant 0\ \forall p_k, \mathbf{p}_{-k}$ and $0 < \theta_k < 1$, we have that the minimum argument to the logarithm operation is 1, which guarantees the continuity of the utility function.

Condition C1 is proven as discussed in [27]. Because the strategy set $\mathcal{A}_k$ is a segment of the real line, given by $[0, P_{\max}]$, it follows that it is non-empty, convex and compact.

With those considerations, we demonstrated the necessary conditions and prove the existence of the Nash equilibrium in the game proposed. To discuss the achieved equilibriums, we consider the possible values for the two proposed algorithms.

After the execution of Algorithm 1 and convergence of the Verhulst PCA, we have the power vector $\mathbf{p}$, with $p_k \in [0, P_{\max}],\ \forall k$, which denotes the allocated power for all users. Because this algorithm only accept users operating at the maximum EE, it checks if the first derivative of u_k (defined in Equation (20)) is equal to zero, corresponding to the maximiser point, because the kth utility function is strictly quasiconcave. Then, there are two possibilities:

(1) if $[u_k(p_k, \mathbf{p}_{-k})]' = 0$ for all users, then all of them operate at the maximum EE and the equilibrium p is a Nash equilibrium, and $p_k = p_k^*, \forall k$.
(2) if $[u_k(p_k, \mathbf{p}_{-k})]' \neq 0$ for one or more users, then those users are grouped into an outage group (K_{out}). Hence, one user belonging to this group is removed from the system ($p_i = 0$) and inserted in the removed users group list (K_{rem}). After that, the remaining users at K_{out} are reinserted in the system, and the algorithm is restarted. After the exclusion of some users, the condition $[u_k(p_k^*, \mathbf{p}_{-k}^*)]' = 0$ for all the remaining users will occur, and at this point, the equilibrium is also a Nash equilibrium, but now with

$$p_k^* = \begin{cases} p_k, & \text{if } [u_k(p_k, \mathbf{p}_{-k})]' = 0 \\ 0 & \text{if } k \in K_{\text{rem}} \end{cases}$$

For Algorithm 2, after the convergence, we have power vector $\mathbf{p}$, with $p_k \in [0, P_{\max}],\ \forall k$, which denotes the allocated power for all users. Again, to check if users achieved the maximum efficiency, the first derivative of u_k is computed. If $[u_k(p_k, \mathbf{p}_{-k})]' = 0$ for all users, then we have $u_k(p_k, \mathbf{p}_{-k}) > u_k(\grave{p}_k, \mathbf{p}_{-k}), \forall k$, with $\grave{p}_k \in [0, P_{\max})$, and $\mathbf{p}$ is a Nash equilibrium, with $p_k^* = p_k, \forall k$. When $[u_k(p_k, \mathbf{p}_{-k})]' \neq 0$ for one or more users, a second criterion is analysed: if the achieved rate satisfies the minimum rate ($r_k \geqslant r_{k,\min}$), then $p_k = P_{\max}$. In this case, $\mathbf{p}$ is also a Nash equilibrium, because $p_k^* > P_{\max}$ and $u_k(p_k, \mathbf{p}_{-k})$ is strictly quasiconcave, $P_{\max}$ is located in the increasing interval, which means that $u_k(P_{\max}, \mathbf{p}_{-k}) > u_k(\grave{p}_k, \mathbf{p}_{-k})$. For the users that cannot achieve neither maximum efficiency nor the minimum rate, the procedure is the same as that described for case (2) of Algorithm 1. After removing some users, the equilibrium achieved is also a Nash equilibrium, and p_k^* has three possible values:

$$p_k^* = \begin{cases} p_k, & \text{if } [u_k(p_k, \mathbf{p}_{-k})]' = 0 \\ P_{\max}, & \text{if } [u_k(p_k, \mathbf{p}_{-k})]' \neq 0 \text{ and } r_k \geqslant r_{k,\min} \\ 0 & \text{if } k \in K_{\text{rem}} \end{cases}$$

Given that discussion, we prove that our proposed game presents a Nash equilibrium, and the allocated power vector $\mathbf{p}^*$ depends on the chosen algorithms, as described in Theorem 1. □

Uniqueness and Pareto optimality of the Nash equilibrium for the two proposed non-cooperative games

Proof. In the cases in which the equilibrium is achieved without putting any user in outage, the strict quasiconcavity and the one-by-one mapping between power and SINR [7] ensure that no user is able to unilaterally improve his own utility with any other power level $p_k \neq p_k^*$.

For the cases in which users are put in outage, the possibility of multiple equilibriums occurs because it is highly probable that two distinct users have different impacts on the system interference level, because the fading channel conditions are statistically independent, and removing one user without a deterministic and well-defined criterion can make the two algorithms present a non-deterministic game equilibrium. In order to guarantee the equilibrium uniqueness for the two allocation resource algorithms proposed, we defined the following rule to deterministically remove a specific user:

$k_{\text{rem}} = \arg\min_j \{|h_j|,\ \forall j \in K_{\text{out}}\}$;
$K_{\text{rem}} \leftarrow k_{\text{rem}}$ (updating removed users set);
... updating K_{out} set;

With this rule, and the fact that the probability of two users having the same channel gain is close to zero, we can conclude that even for the cases in which it is necessary to remove users, the Nash equilibrium obtained is unique. Hence, the proof for Lemma 2 is completed.

The proof of the Pareto optimality can be found in [9]; the equilibrium obtained with MF detector can be improved if every user decreases the allocated power by a small factor, given the selfish behaviour of the non-cooperative solution. For DEC, because the SINR

achieved, given in Equation (5), does not depend on interfering users power level, the selfish power allocation does not affect the EE. □

ACKNOWLEDGEMENTS

This work was supported in part by the National Council for Scientific and Technological Development (CNPq) of Brazil under grants 202340/2011-2 and 303426/2009-8, the Coordenação de Aperfeiçoamento de Pessoal de Nível Superior (CAPES) and the Londrina State University – Paraná State Government (UEL), Brazil.

REFERENCES

1. Stanczak S, Wiczanowski M, Boche H. *Resource Allocation in wireless networks: Theory and Algorithms*. Springer-Verlag Berlin Heidelberg: Germany, 2006.
2. Meshkati F, Poor HV, Schwartz SC. Energy-efficient resource allocation in wireless networks: an overview of game-theoretic approaches. *IEEE Signal Processing Magazine* 2007; **24**: 58–68.
3. Buzzi S, Poor HV, Zappone A. Transmitter waveform and widely linear receiver design: noncooperative games for wireless multiple-access networks. *Information Theory, IEEE Transactions on* 2010; **56**(10): 4874–4892.
4. Miao G, Himayat N, Li Y. Energy-efficient link adaptation in frequency-selective channels. *IEEE Transactions on Communication* 2010; **58**(2): 545–554.
5. Han C, Harrold T, Armour S, Krikidis I, Videv S, Grant PM, Haas H, Thompson JS, Ku I, Wang C-X, Le TA, Nakhai MR, Zhang J, Hanzo L. Green radio: radio techniques to enable energy-efficient wireless networks. *Communications Magazine, IEEE* 2011; **49**(6): 46–54.
6. Miao G, Himayat N, Li GY, Talwa S. Low-complexity energy-efficient OFDMA, Communications, 2009. ICC '09. IEEE international conference on, 2009; 1–5.
7. Meshkati F, Poor H, Schwartz S, Mandayam N. An energy-efficient approach to power control and receiver design in wireless data networks. *Communications, IEEE Transactions on* 2005; **53**(11): 1885–1894.
8. Buzzi S, Poor H. Joint receiver and transmitter optimization for energy-efficient CDMA communications. *Selected Areas in Communications, IEEE Journal on* 2008; **26**(3): 459–472.
9. Betz S, Poor H. Energy efficiency in multi-hop CDMA networks: a game theoretic analysis considering operating costs, In *Icassp'08 - ieee international conference on acoustics, speech and signal processing*, Las Vegas, USA: IEEE, 2008; 2781–2784.
10. Chen Y, Zhang S, Xu S, Li G. Fundamental trade-offs on green wireless networks. *Communications Magazine, IEEE* 2011; **49**(6): 30–37.
11. Miao G, Himayat N, Li G, Talwar S. Distributed interference-aware energy-efficient power optimization. *Wireless Communications, IEEE Transactions on* 2011; **10**(4): 1323–1333.
12. Ozel O, Uysal-Biyikoglu E. Network-wide energy efficiency in wireless networks with multiple access points. *Transactions on Emerging Telecommunications Technologies* 2012: n/a–n/a. (available from: http://dx.doi.org/10.1002/ett.2543).
13. Zhang X, Zhang J, Huang Y, Wang W. On the study of fundamental trade-offs between QoE and energy efficiency in wireless networks. *Transactions on Emerging Telecommunications Technologies* 2013; **24**(3): 259–265. (Available from: http://dx.doi.org/10.1002/ett.2640).
14. Saraydar C, Mandayam N, Goodman D. Efficient power control via pricing in wireless data networks. *IEEE Trans. Commun.* 2002; **50**(2): 291–303.
15. Fudenberg D, Tirole J. *Game Theory*. MIT Press: USA, 1991.
16. Sampaio LDH, Lima MF, Zarpelão BB, Proença ML, Abrão T. Power allocation in multirate DS/CDMA systems based on Verhulst equilibrium, In *IEEE ICC 2010 - Communication Qos, Reliability and Modeling Symposium*, Cape Town, South Africa: IEEE, 2010; 1–6.
17. Meshkati F, Chiang M, Poor HV, Schwartz SC. A game-theoretic approach to energy-efficient power control in multicarrier CDMA systems. *Selected Areas in Communications, IEEE Journal on* 2006; **24**(6): 1115 –1129.
18. Nagarajan V, Dananjayan P. A novel game theoretic approach for energy efficient modulation in MC-DS-CDMA, In *Future Computer And Communication, 2009. ICFCC 2009. International Conference on*, 2009; 112 –116.
19. Lupas R, Verdu S. Linear multiuser detectors for synchronous code-division multiple-access channels. *IEEE Transactions on Information Theory* 1989; **1**: 123–136.
20. Shannon CE. A mathematical theory of communication. *Bell System Technical Journal* 1948; **27**: 379–423 and 623–656.
21. Goldsmith A, Varaiya P. Capacity of fading channel with channel side information. *IEEE Transactions on Information Theory* 1995; **43**: 1986–1992.
22. Tse D, Viswanath P. *Fundamentals of Wireless Communications*, 1st ed. Cambridge University Press: UK, 2010.
23. Goldsmith AJ, Chua SG. Variable-rate variable-power MQAM for fading channels. *IEEE Transactions on Communications* 1997; **45**(10): 1218–1230.
24. Goodman DJ, Mandayan NB. Power control for wireless data. *IEEE Personal Communication Magazine* 2000; **7**(4): 48–54.

25. Rodriguez V. An analytical foundation for resource management in wireless communication. *Global telecommunications conference, 2003. globecom'03. ieee* 2003; **2**: 898–902.
26. Gross TJ, Abrão T, Jeszensky PJE. Distributed power control algorithm for multiple access systems based on Verhulst model. *AEU - International Journal of Electronics and Communications* 2011; **65**(4): 361 –372.
27. Buzzi S, Saturnino D. A game-theoretic approach to energy-efficient power control and receiver design in cognitive CDMA wireless networks. *Selected Topics in Signal Processing, IEEE Journal of* 2011; **5**(1): 137 –150.